


2011

# Characterization of Heterogeneities and Domains in Aquatic and Sedimentary Organic Matter by $^1\text{H}$ Spin Diffusion: Potential for Elucidating the Formation Mechanisms

Jingdong Mao  
*Old Dominion University*

Xiaoyan Cao  
*Old Dominion University*

Follow this and additional works at: [https://digitalcommons.odu.edu/chemistry\\_fac\\_pubs](https://digitalcommons.odu.edu/chemistry_fac_pubs)

 Part of the [Chemistry Commons](#), [Fresh Water Studies Commons](#), [Marine Biology Commons](#), and the [Oceanography Commons](#)

## Repository Citation

Mao, Jingdong and Cao, Xiaoyan, "Characterization of Heterogeneities and Domains in Aquatic and Sedimentary Organic Matter by  $^1\text{H}$  Spin Diffusion: Potential for Elucidating the Formation Mechanisms" (2011). *Chemistry & Biochemistry Faculty Publications*. 119.  
[https://digitalcommons.odu.edu/chemistry\\_fac\\_pubs/119](https://digitalcommons.odu.edu/chemistry_fac_pubs/119)

## Original Publication Citation

Mao, J. D., & Cao, X. Y. (2011). Characterization of heterogeneities and domains in aquatic and sedimentary organic matter by  $^1\text{H}$  spin diffusion: Potential for elucidating the formation mechanisms. *Limnology and Oceanography: Methods*, 9, 533-542. doi:10.4319/lom.2011.9.533

## Characterization of heterogeneities and domains in aquatic and sedimentary organic matter by $^1\text{H}$ spin diffusion: Potential for elucidating the formation mechanisms

Jingdong Mao\* and Xiaoyan Cao

Department of Chemistry and Biochemistry, Old Dominion University, 4541 Hampton Blvd, Norfolk, Virginia 23529, USA

### Abstract

Although the information on domains and heterogeneities of natural organic matter (NOM) can provide insights into its formation mechanisms, the appropriate solid-state NMR technique for measuring them is still lacking. The traditional technique requires mobility differences in NOM whereas NOM components are primarily rigid. We introduced a new  $^1\text{H}$  spin diffusion technique,  $^1\text{H}$ - $^{13}\text{C}$  two-dimensional heteronuclear correlation (2D HETCOR) NMR with  $^1\text{H}$  spin diffusion, for characterization of domains and heterogeneities in aquatic and sedimentary organic matter. It was achieved by collecting a series of 2D HETCOR spectra with a variable mixing time,  $t_m$ , and monitoring the transfer of magnetization from one component to another. The rate of magnetization transfer provided the information on domains and heterogeneities because the magnetization of small domains or heterogeneities equilibrated faster than that of larger ones. Three samples, International Humic Substances Society (IHSS) Suwannee River NOM, IHSS Suwannee River humic acid (HA), and a sedimentary HA, were used. Two model polymers, a random copolymer poly(styrene-*n*-butyl methacrylate) with 0.6-nm heterogeneity and a block copolymer polystyrene-*b*-poly(methyl methacrylate) with a domain size of 5 nm, were included for calibration. Within  $t_m < 100 \mu\text{s}$ , half equilibration was reached for all three NOM samples and poly(styrene-*n*-butyl methacrylate), indicating that they were heterogeneous. In contrast, the spin diffusion of polystyrene-*b*-poly(methyl methacrylate) with 5-nm domain was much slower. Unlike the traditional spin diffusion technique, this technique did not require the differential mobility in NOM and was suitable for investigating the domains and heterogeneities of NOM, which are mostly rigid.

Natural organic matter (NOM) is ubiquitous in the environment. NOM in water controls a number of important physical, chemical, and biological processes in aquatic environments. For example, it impacts the global carbon cycle and plays a significant role in carbon sequestration and global warming. It influences metal speciation and bioavailability, and transport and fate of organic xenobiotics. Under many circumstances, especially in freshwater systems, aquatic NOM functions as the major buffering system and has serious implications for the acidification of rivers, lakes, and oceans (Hedges et al. 2000; Cook 2004). Characterization of organic matter in natural

waters and sediments is fundamental to the understanding of its origins, compositions, functions, and cycling. Despite the extensive efforts to investigate the structures of organic matter using various techniques for many years, a large fraction of this material is not well characterized (Wakeham et al. 1997; Hedges et al. 2000; Schmidt et al. 2009; Gogou and Repeta 2010; Stephens and Minor 2010), and its formation mechanisms are still unclear. Solid-state nuclear magnetic resonance (NMR) spectroscopy is considered as one of the best techniques for characterizing the structures of aquatic and sedimentary organic matter (Pines et al. 1973; Mehring 1983; Botto et al. 1987; Preston 1996; Nanny et al. 1997; Conte and Piccolo 1999; Hatcher et al. 2001; Cook 2004; Conte et al. 2004; Abdulla et al. 2010). The most frequently used solid-state NMR technique is  $^{13}\text{C}$  cross polarization/magic angle spinning (CP/MAS). Although applications of this technique have significantly advanced our understanding of aquatic and sedimentary organic matter, it suffers from drawbacks such as low cross polarization efficiency for some segments such as mobile groups, and thus can only provide semi-quantitative structural information. Moreover, the  $^{13}\text{C}$  CP/MAS spectra of

\*Corresponding author: E-mail: jmao@odu.edu

### Acknowledgments

We thank the National Science Foundation (EAR-0843996, CBET-0853950, and DEB-1057472) and the Thomas F. Jeffress and Kate Miller Jeffress Memorial Trust for financial support. We also thank Prof. Klaus Schmidt-Rohr for his kind support and Profs. Paul R. Bloom, C. Edward Clapp, Luc Tremblay, and Jean-Pierre Gagné for kindly providing NOM samples.

almost all aquatic and sedimentary organic matter are broad due to many different chemical species that are present, and therefore it is difficult to identify specific functional groups from these overlapping spectra.

Recent advances in solid-state NMR techniques, developed especially for characterization of NOM, have shown the promise of significantly improving our understanding of its structures (Mao et al. 2007a; Mao et al. 2007b; Mao et al. 2010). These systematic techniques allow us to identify specific functional groups, obtain quantitative structural information, detect connectivities and proximities, and examine domains and heterogeneities. In contrast to  $^{13}\text{C}$  CP/MAS technique, which can only identify approximately 10 types of functional groups in NOM due to broad and heavily overlapping spectra, the systematic, advanced solid-state NMR techniques can be employed to detect many more specific functional groups and moieties in NOM. In particular, the recently introduced spectral-editing techniques can selectively retain certain signals and eliminate others, clearly revealing specific functional groups (Schmidt-Rohr and Mao 2002; Mao and Schmidt-Rohr

2004; Mao and Schmidt-Rohr 2005; Mao and Schmidt-Rohr 2006). We can also use two-dimensional  $^1\text{H}$ - $^{13}\text{C}$  heteronuclear correlation (2D HETCOR) NMR to detect the proximities and connectivities of different functional groups. With the information provided by these systematic, advanced solid-state NMR techniques, then the next questions would be "How homogeneous is NOM?" and "Are there domains or just heterogeneities in NOM?"

In NOM, both chemical and physical domains can be present. The domains of crystalline and amorphous poly(methylene) found in humic substances belong to physical domains (Hu et al. 2000). Chemical domains, such as lignin and polysaccharide domains, refer to the same kinds of chemical compounds associated together with certain sizes (Fig. 1). The terminology of "domain" is usually used to depict those regions with diameters more than 5 nm; otherwise, "heterogeneity" is employed if the diameters are less than 5 nm (Schmidt-Rohr and Spiess 1994). Fig. 1a shows the schematics of polysaccharide and lignin domains. Sugar rings or lignin units are associated together, with sizes more than 5 nm. In contrast, in Fig.

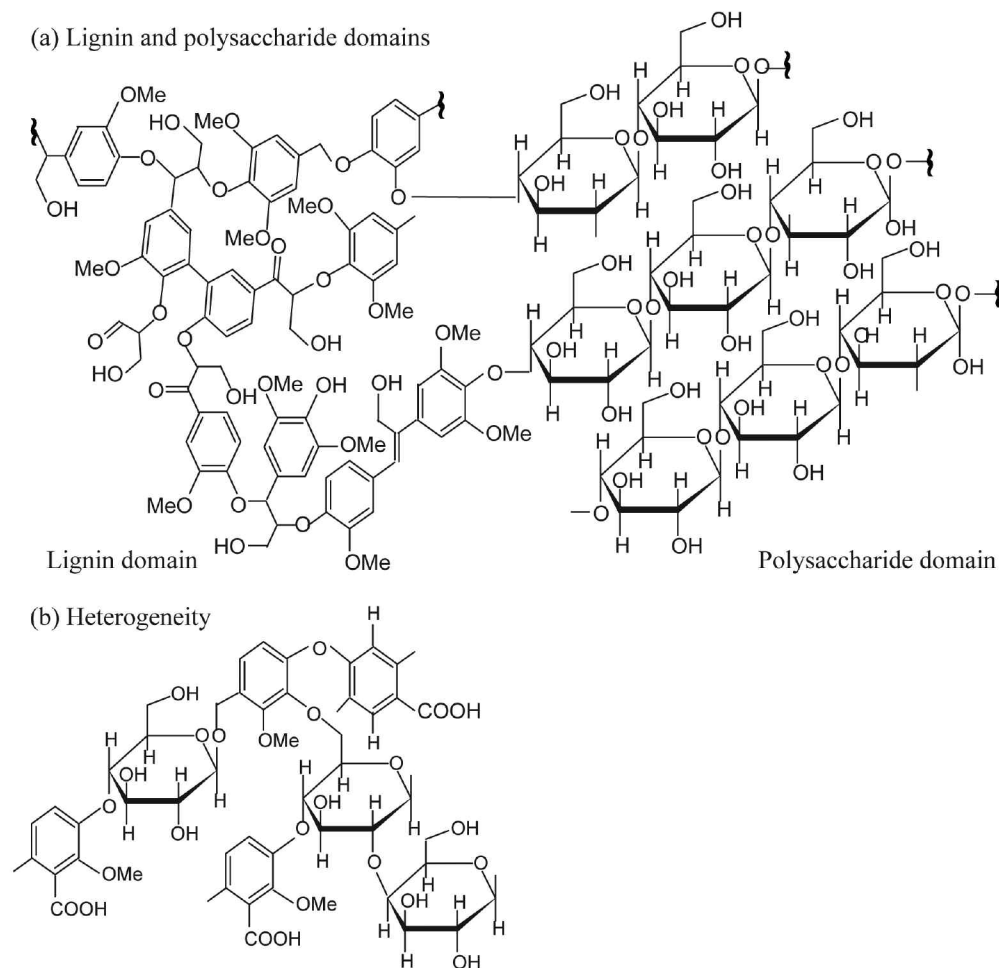


**Fig. 1.** Schematics showing the concepts of domain and heterogeneity. (a) Lignin units or sugar rings associated together are large enough to become lignin and polysaccharide domains. (b) Sugar rings and lignin units are randomly connected so that only heterogeneity is present.

1b the monomers of sugars and lignin structural units are randomly bonded together, leading to "heterogeneity." The nanometer-scale chemical heterogeneity or domain of NOM is its important structural aspect and has significant implications. Especially, it can provide insights into the formation of NOM. There are two major hypotheses for the formation of NOM: the decomposition of biopolymers into short oligomers, followed by random repolymerization (Stevenson 1994), and preservation of residual biopolymers such as refractory cutan, cutin, suberan, and suberin (Philp and Calvin 1976; Hatcher et al. 1983). Partial survival of biomacromolecules such as lignin, polysaccharides, and proteins would result in domains or heterogeneities on a  $> 1$ -nm scale, whereas depolymerization-repolymerization could lead to the intimate mixing of components and therefore heterogeneities  $< 1$  nm. Therefore, if we can measure the domains and heterogeneities in NOM, then we can clarify the formation mechanisms of NOM to a certain extent.

Nevertheless, the information on domains and heterogeneities of NOM is still unclear due to lack of appropriate techniques. The frequently used solid-state NMR technique for investigation of domains and heterogeneities in polymer science is Goldman-Shen spin diffusion (Schmidt-Rohr and Spiess 1994). Similar to typical exchange NMR experiments, spin diffusion consists of three periods including selection, mixing time  $t_m$ , and detection. To perform a  $^1\text{H}$  spin diffusion experiment, a spatially inhomogeneous distribution of  $z$  magnetization is usually generated first and  $^1\text{H}$  spin diffusion is introduced during the mixing time. The magnetization of small domains or heterogeneities equilibrates faster than that of larger ones. However, the limitation of Goldman-Shen spin diffusion technique is that it requires differential component mobility in a sample (Mao et al. 2007b). Therefore, Goldman-Shen spin diffusion technique is not widely applicable to NOM considering that the components of most aquatic NOM samples are rigid. To overcome this limitation, a new  $^1\text{H}$  spin diffusion technique that does not require the presence of rigid and mobile groups in a sample must be developed. In the present study, we introduce a new  $^1\text{H}$  spin diffusion technique,  $^1\text{H}$ - $^{13}\text{C}$  2D HETCOR combined with  $^1\text{H}$  spin diffusion, to estimate the domains or heterogeneities in NOM. In this technique, a series of 2D HETCOR spectra with a variable mixing time,  $t_m$ , are collected, and the  $^{13}\text{C}$  slices extracted at a certain proton site from these 2D HETCOR spectra allow for monitoring the transfer of magnetization from one component to another. The magnetization transfer rate provides the information on domains and heterogeneities on NOM.

## Materials and procedures

### Samples

Three NOM samples were employed in the present study. The two aquatic organic matter samples were (a) International Humic Substances Society (IHSS) Suwannee River natural organic matter, RO isolation (Cat. #1R101N), and (b) IHSS

Suwannee River humic acid (HA), Standard II (#2S101H). Both were kindly provided by Dr. Paul R. Bloom, University of Minnesota, St. Paul. The details of the two standard samples can be found on the IHSS homepage ([www.ihss.gatech.edu/](http://www.ihss.gatech.edu/)).

In addition, an HA sample from the sediment of the Saguenay Fjord near the Saguenay River end-member was used. It was kindly provided by Dr. Luc Tremblay, Université de Moncton, Canada. The Saguenay Fjord is the most important tributary of the St. Lawrence Estuary. The sediment was collected using a  $0.06\text{ m}^2$  Hessler-type box corer (Tremblay and Gagne 2007) and was sub-sampled from the first centimeter of the box cores under a  $\text{N}_2$  atmosphere in a glove-box on-board ship. The sub-sample was kept frozen in the dark until freeze-drying. The extraction of HAs was performed using the method adopted by IHSS (Swift 1996). The HA sample was freeze-dried before NMR analyses. Other information on this sedimentary HA such as elemental composition was described elsewhere (Tremblay and Gagne 2007). For calibration, a 50:50 block copolymer polystyrene-*b*-poly(methyl methacrylate) (PS-*b*-PMMA) with a 5-nm domain size and a synthetic random copolymer poly(styrene-*n*-butyl methacrylate) (poly(styrene-*n*BMA)) with only heterogeneity around 0.6 nm were included. They were purchased from Scientific Polymer Products. The information on their domain and heterogeneity has been described in the literature (Clauss et al. 1993; Mao and Schmidt-Rohr, 2006).

### $^{13}\text{C}$ NMR spectroscopy

All the experiments were performed on a Bruker DSX400 spectrometer at 100 MHz for  $^{13}\text{C}$ . Seven-millimeter sample rotors in a double-resonance probe head were used for best sensitivity.

### $^{13}\text{C}$ cross polarization and total suppression of sidebands (CP/TOSS) and $^{13}\text{C}$ CP/TOSS plus dipolar dephasing

Semi-quantitative compositional information was obtained with good sensitivity using a  $^{13}\text{C}$  CP/MAS NMR technique (MAS = 6.5 kHz, CP time = 1 ms, and  $^1\text{H}$   $90^\circ$  pulse-length = 4  $\mu\text{s}$ ). Four-pulse total suppression of sidebands (TOSS) (Dixon 1982) was employed before detection, with the two-pulse phase-modulated (TPPM) decoupling applied for optimum resolution. Sub-spectra for nonprotonated and mobile carbon groups were obtained by combining the  $^{13}\text{C}$  CP/TOSS sequence with a 40- $\mu\text{s}$  dipolar dephasing.

### $^{13}\text{C}$ chemical-shift-anisotropy (CSA) filter

The O-C-O carbons (e.g., anomeric C in carbohydrate rings) and aromatic carbon resonances can overlap between 120 and 90 ppm. The aromatic carbon signals were selectively suppressed using a five-pulse  $^{13}\text{C}$  CSA filter with a CSA-filter time of 35  $\mu\text{s}$  (Mao and Schmidt-Rohr 2004).

### Immobile protonated-only

Signals of immobile  $\text{CH}_2$  and CH groups can be selected with good sensitivity in a simple spectral-editing experiment. Two spectra are recorded. The first is a CP/TOSS spectrum with a short CP of 50  $\mu\text{s}$ ; the second a CP/TOSS spectrum with a short CP of 50  $\mu\text{s}$  and 40  $\mu\text{s}$  dipolar dephasing. The first spec-

trum is predominantly composed of signals from protonated carbons in immobile segments, with some residual signals of quaternary carbons resulting from two-bond magnetization transfer. The second one contains only the residual signals of quaternary carbons ( $C_q$ ) or mobile segments (including  $CH_3$  groups with > 50% efficiency). The difference of the two spectra yields the spectrum of the immobile  $CH_2$  and  $CH$  carbons, with a small  $CH_3$  contribution.

### $^1H$ spin diffusion

The pulse sequence of the  $^1H$ - $^{13}C$  2D HETCOR NMR with  $^1H$  spin diffusion is shown in Fig. 2a. Like typical 2D NMR pulse sequence, it consists of preparation, evolution, mixing, and detection, with two frequency dimensions,  $^1H$  chemical shift  $\omega_1$  and  $^{13}C$  chemical shift  $\omega_2$ . In 1D Fourier transform NMR signals are recorded as a function of one time variable and the resulting data Fourier transformed to generate a spectrum of a function of only one frequency variable. In 2D NMR signals are collected as a function of two time variables,  $t_1$  and  $t_2$ , and then Fourier transformed two times to produce a spectrum of a function of two frequency variables. The general scheme for 2D NMR is preparation, evolution ( $t_1$ ), mixing, and detection ( $t_2$ ). In the preparation period, samples are excited by pulses (or a pulse) and the resulting magnetization evolves during evolution time ( $t_1$ ), which is a variable delay time. The next period is the mixing time. Finally, signals are detected as a function of the second time variable,  $t_2$ . A series of free induction decays (FIDs) are repeatedly acquired during  $t_2$  with the  $t_1$  interval increased by a uniform amount each time. Subjecting each of the acquired  $t_2$  FIDs to double Fourier transformation with respect to first  $t_2$  and then  $t_1$ , produces the two frequencies ( $\omega_1$  and  $\omega_2$ ) of a 2D NMR spectrum.

The pulse sequence of Fig. 2a starts with a  $90^\circ$   $^1H$  pulse. After the excitation, frequency-switched Lee-Goldburg (FSLG) homonuclear decoupling during  $t_1$  (corresponding to  $^1H$  chemical shift  $\omega_1$  after Fourier transformation) is followed. Then two pulses (one  $54.7^\circ$  and another  $90^\circ$ ) are employed to put magnetization to  $z$  axis, followed by the mixing time  $t_m$  where  $^1H$  spin diffusion occurs since  $^1H$  spin diffusion is the diffusion of  $^1H$   $z$  magnetization. Afterward, a  $54.7^\circ$   $^1H$  pulse puts its magnetization at the magic angle for Lee-Goldburg cross polarization (LG-CP). In this technique, a short 80- $\mu s$  LG-CP time is used to minimize spin diffusion during this period. To suppress sidebands the  $^{13}C$  four-pulse TOSS is employed before detection, and TPPM decoupling is applied during  $^{13}C$  detection for optimum resolution. A series of  $^1H$ - $^{13}C$  2D HETCOR spectra with various spin diffusion times,  $t_m$  (usually about 10 mixing times ranging from 5  $\mu s$  to 10 ms), are collected. 2D HETCOR is used to identify (1) the origin of magnetization by  $^1H$  chemical shift ( $\omega_1$ ) and (2) the final location of magnetization by  $^{13}C$  chemical shift ( $\omega_2$ ) (Fig. 3). Figs. 3a and 3b are the 2D HETCOR spectra without spin diffusion ( $t_m = 5 \mu s$ ) and with a mixing time of 200  $\mu s$ , respectively. The  $\omega_1$  dimension (y axis) shows the  $^1H$  chemical shift whereas the  $\omega_2$  dimension (x axis) is the  $^{13}C$  chemical shift. Usually, contour plotting is used for the dis-

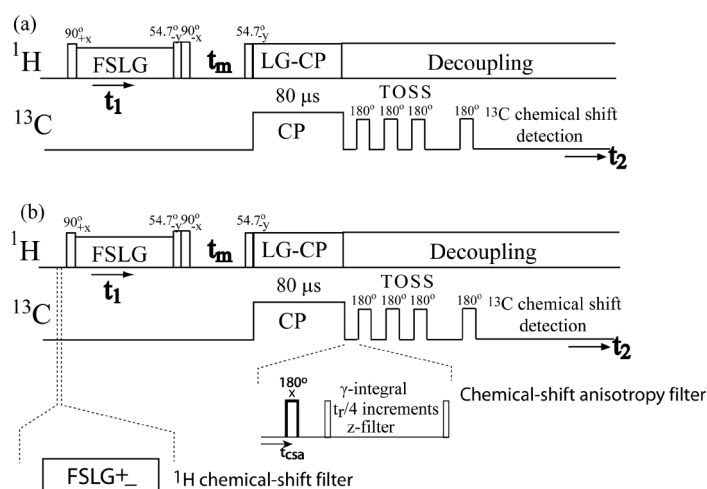


**Fig. 2.** (a) Pulse sequence of the new  $^1H$  spin diffusion technique of 2D HETCOR with  $^1H$  spin diffusion for examining domains and heterogeneities. (b) Revised pulse sequence showing the insertion of  $^1H$  chemical-shift filter before  $90^\circ$   $^1H$  pulse in the proton channel or the insertion of  $^{13}C$  chemical-shift filter before TOSS in the  $^{13}C$  channel. These filter techniques contribute to clean selection of a specific functional group and assist the quantitative estimation of  $^1H$  spin diffusion. See text for further details.

play of 2D HETCOR spectra. The “diagonal” signals illustrate primarily the correlations of carbons directly bonded with their own protons (i.e., aromatic carbons with aromatic protons) whereas “off-diagonal” signals display the correlations of carbons and protons, which are not directly bonded. To observe the transfer of aromatic magnetization, the  $^{13}C$  slices are extracted at  $^1H$  chemical shift of ca. 7.5 ppm. Without  $^1H$  spin diffusion, we mostly observe diagonal signals showing the correlations of carbons with their directly bonded protons. That is, the carbon slice extracted at the aromatic  $^1H$  chemical shift of ca. 7.5 ppm without  $^1H$  spin diffusion primarily shows aromatic  $^{13}C$  magnetization (Fig. 3c). With the introduction of 200- $\mu s$  mixing time ( $t_m$ ) or  $^1H$  spin diffusion time, cross peaks between different functional groups appear and the carbon slice not only shows dominant aromatic bands but also other signals such as those of aliphatics (Fig. 3d). The comparison of the carbon slices of Figs. 3c and 3d clearly shows the magnetization transfer from aromatics to other functional groups. Based on this, we can observe the rate of magnetization transfer, i.e.,  $^1H$  spin diffusion rate and how fast the equilibration of magnetization can be reached. For heterogeneities less than 1 nm, fast equilibration (<1 ms) is expected whereas for domains slow equilibration occurs. For large domains (>20 nm), no equilibration can be reached before  $^{13}C$   $T_1$  relaxation dephases the signals. Unlike the Goldman-Shen technique, this technique does not require the presence of distinct mobile and rigid components in NOM to identify domains or heterogeneities. The rate of this magnetization transfer can be used to estimate the sizes of domains and heterogeneities.

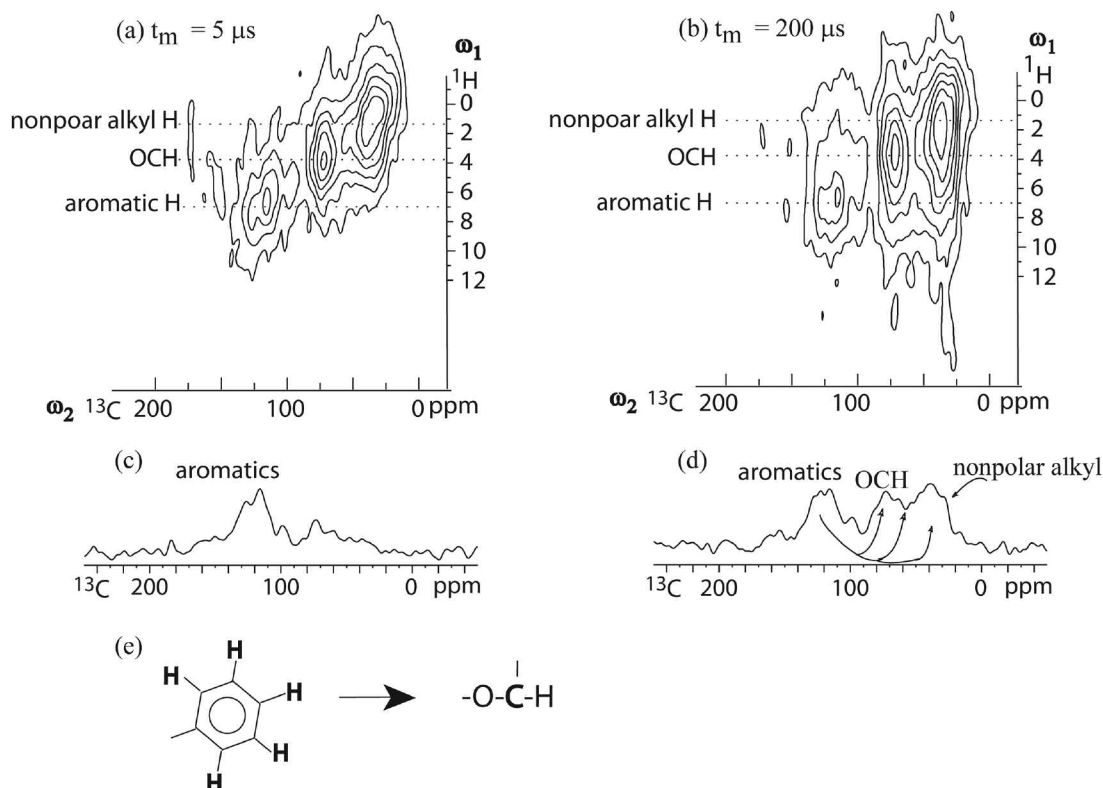


**Fig. 3.** Two  $^1\text{H}$ - $^{13}\text{C}$  2D HETCOR spectra of IHSS Suwannee River HA used to demonstrate the basic principle of the spin diffusion technique. (a) 2D HETCOR spectra without spin diffusion ( $t_m = 5 \mu\text{s}$ ). (b) 2D HETCOR with a mixing time of  $200 \mu\text{s}$ . To observe the transfer of aromatic magnetization, the  $^{13}\text{C}$  slices are extracted at  $^1\text{H}$  chemical shift of ca. 7.5 ppm. (c)  $^{13}\text{C}$  slice of 2D HETCOR spectrum (a) and selection of aromatic magnetization is achieved. (d)  $^{13}\text{C}$  slice of 2D HETCOR spectrum (b) and the transfer of magnetization from aromatics to other functional groups occur significantly. (e) Schematic showing the transfer of the magnetization from aromatic protons to OCH carbons.

To analyze the data quantitatively for the aromatic-proton cross sections, the intensity of one functional group (i.e., OCH of carbohydrates) is integrated and the spin-diffusion curve showing integrals obtained at different mixing times versus  $t_m^{1/2}$  is plotted. The aromatic and OCH proton resonances, whose separation is usually sufficient for obtaining cross peaks with < 20% contributions arising from wings of strong peaks at other proton chemical shifts, are focused on (Fig. 3e). To obtain approximate sizes of domains or heterogeneities, model compounds with known sizes of domains or heterogeneities are included and their spin-diffusion curves are used for calibration.

### Assessment

Three NOM samples, IHSS Suwannee River NOM and HA, and Fjord sedimentary HA, are used to demonstrate our method for estimating domains and heterogeneities in NOM. We primarily focus on IHSS Suwannee River HA (Figs. 4-7). But we show the spin-diffusion curves of all the samples, including those of two model polymers used for calibration (Fig. 7). In the assessment, we first use spectral-editing techniques to show that there are lignin and carbohydrate residues in IHSS

Suwannee River HA. Then we use the  $^1\text{H}$  spin diffusion technique to address whether these lignin and carbohydrate residues form domains or exhibit just heterogeneity.

### Presence of lignin and carbohydrate residues in IHSS Suwannee River HA based on spectral-editing techniques

Fig. 4 shows the spectra of  $^{13}\text{C}$  CP/TOSS and several spectral-editing techniques such as dipolar dephasing, protonated-carbon-only, and  $^{13}\text{C}$  chemical shift anisotropy. The  $^{13}\text{C}$  CP/TOSS spectrum (Fig. 4a) indicates that this HA, like typical NOM samples, is chemically complex. Signals are heavily overlapped and observed within the whole range of 0-220 ppm. Dipolar-dephased spectrum (Fig. 4b) displays signals of  $\text{CCH}_3$  around 24 ppm,  $\text{CC}_q$  ( $\text{C}_q$ , quaternary carbon) around 40 ppm,  $\text{OCH}_3$  groups at 56 ppm,  $\text{OC}_q$  from 70-95 ppm,  $\text{OC}_q\text{O}$  around 100 ppm, nonprotonated aromatics around 110 and 130 ppm, aromatic C-O around 150 ppm,  $\text{COO}/\text{N}-\text{C}=\text{O}$  groups around 172 ppm, and ketones and aldehydes around 200 ppm. The protonated-only spectrum shows residual  $\text{CCH}_3$  between 0-24 ppm,  $\text{CCH}_2\text{C}$  around 30 ppm, OCH around 72 ppm, OCHO around 100 ppm, and aromatic C-H around 115 and 130 ppm. The  $^{13}\text{C}$  CSA-filtered spectrum clearly shows the presence of OCO resonances around 108 ppm. This OCO sig-

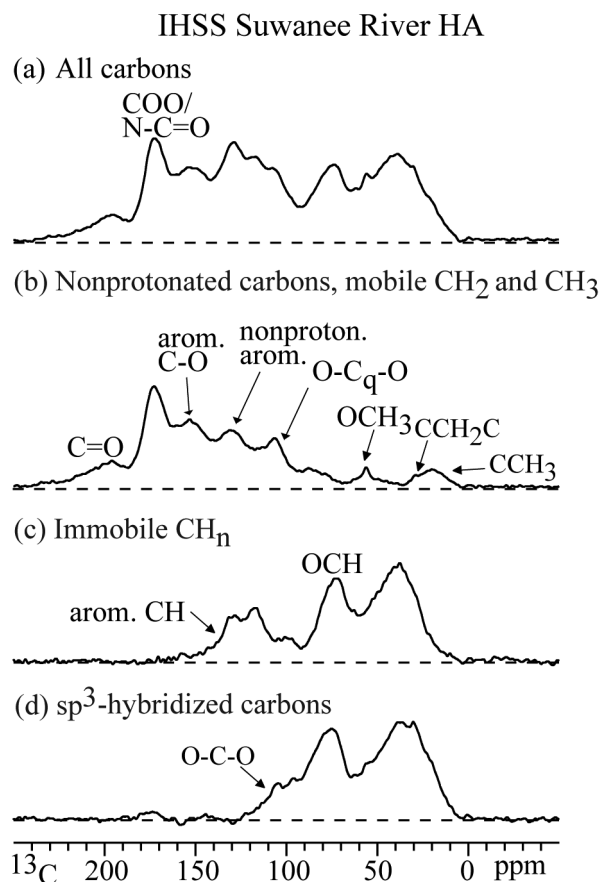


**Fig. 4.** Simple spectral-editing spectra of IHSS Suwannee River HA: (a)  $^{13}\text{C}$  CP/TOSS showing the qualitative structural information, (b) dipolar-depased spectrum showing nonprotonated carbons and carbons of mobile groups such as  $\text{CH}_3$  groups, (c) protonated-carbon-only spectrum showing only immobile protonated carbons, (d)  $^{13}\text{C}$  CSA-filtered spectrum showing only  $\text{sp}^3$ -hybridized carbons.

nal plus OCH resonance around 72 ppm are indicative of the presence of carbohydrates or carbohydrate residues in this HA. The signals of aromatic C-O, aromatics, and  $\text{OCH}_3$  around 150, 130, and 56 ppm indicate that lignin or lignin residues are present in this sample. With this structural information, then the following question “Do these carbohydrate or lignin residues form domains or they are just of heterogeneity?” would arise. The answer to this question has important implications for the formation mechanisms of NOM, as above mentioned. This question can be addressed by the 2D HETCOR with  $^1\text{H}$  spin diffusion technique.

#### Collection of a series of 2D HETCOR spectra with different mixing times

Fig. 5 shows a series of  $^1\text{H}$ - $^{13}\text{C}$  2D HETCOR spectra with mixing times  $t_m$  of 5  $\mu\text{s}$ , 10  $\mu\text{s}$ , 20  $\mu\text{s}$ , 50  $\mu\text{s}$ , 100  $\mu\text{s}$ , 200  $\mu\text{s}$ , 500  $\mu\text{s}$ , 1 ms, 2 ms, 5 ms, and 10 ms. At  $t_m = 5 \mu\text{s}$  without  $^1\text{H}$  spin diffusion introduced, only one-bond  $^1\text{H}$ - $^{13}\text{C}$  correlations, for example, those between aromatic protons and carbons, are observed, showing only the diagonal signals, as expected.

Actually, up to  $t_m = 50 \mu\text{s}$  only slight cross peaks are developed. But at  $t_m = 100 \mu\text{s}$  obvious cross peaks start to appear. At  $t_m = 200 \mu\text{s}$ , the 2D HETCOR spectrum has a significantly different pattern, with cross-peak intensity representing the correlations between all types of protons and carbons present. With  $t_m = 1 \text{ ms}$ , almost all the magnetization is equilibrated throughout the whole sample.

Carbon slices at aromatic-proton position, i.e., around 7.5 ppm are then extracted to (1) monitor the magnetization transfer from aromatics to other functional groups more clearly and (2) quantitatively estimate the rate of this magnetization transfer by integration. These carbon slices are shown in Fig. 6. The equilibration slice with  $t_m = \infty$  is also shown on the top of this series of spectra. Clearly, without  $^1\text{H}$  spin diffusion, the dominant  $^{13}\text{C}$  signals are those of aromatics. At  $t_m = 100 \mu\text{s}$ , magnetization equilibration is reached for almost all the functional groups except for that of nonpolar alkyls around 0–50 ppm. At  $t_m = 2 \text{ ms}$ , the magnetization is equilibrated throughout the whole structure.

#### Quantitative $^1\text{H}$ spin diffusion curves

To obtain  $^1\text{H}$  spin-diffusion curves for quantitative analysis, we need to integrate OCH bands around 72 ppm and then plot their intensity changes as a function of  $t_m^{1/2}$  (Fig. 7). In Fig. 7, the spin diffusion curves of IHSS Suwannee River HA, IHSS Suwannee River NOM, and the sedimentary HA are plotted. For calibration, the data of two model synthetic polymers with known domain or just heterogeneity, PS-*b*-PMMA and poly(styrene-*n*BMA), are also included. The 50:50 block copolymer PS-*b*-PMMA has a 5-nm domain size whereas for the synthetic random copolymer poly(styrene-*n*BMA) only heterogeneity around 0.6 nm is present due to the mixing on the length scale of a few bonds. Within  $t_m < 100 \mu\text{s}$ , half equilibration is reached for all three NOM samples and the random copolymer poly(styrene-*n*BMA) with only heterogeneity, but not for 50:50 block copolymer PS-*b*-PMMA of 5-nm domain. The equilibration in the NOM samples occurs on the same time scale as in the random copolymer poly(styrene-*n*BMA) of only heterogeneity, proving only heterogeneities in these samples. In contrast, the spin diffusion data of the 50:50 block copolymer (PS-*b*-PMMA) whose domain size is 5 nm show much slower equilibration of  $^1\text{H}$  magnetization between domains than the spin exchange in NOM samples. This indicates that there are neither polysaccharide domains nor lignin domains but only heterogeneities present in these NOM samples. In this assessment, through the real-world applications, we demonstrate that the new  $^1\text{H}$  spin-diffusion technique works well for investigating domains and heterogeneities in NOM. It does not require the mobility differences in a NOM sample. The setup of this technique is straightforward as long as the potential users have some basic solid-state NMR knowledge. The disadvantage of this technique is that it takes long measurement times. For 2D HETCOR experiments, 7-mm rotors with approximately 150 mg organic matter samples are used. With a recycle delay of 0.5 s, 96  $t_1$  increments, and 832

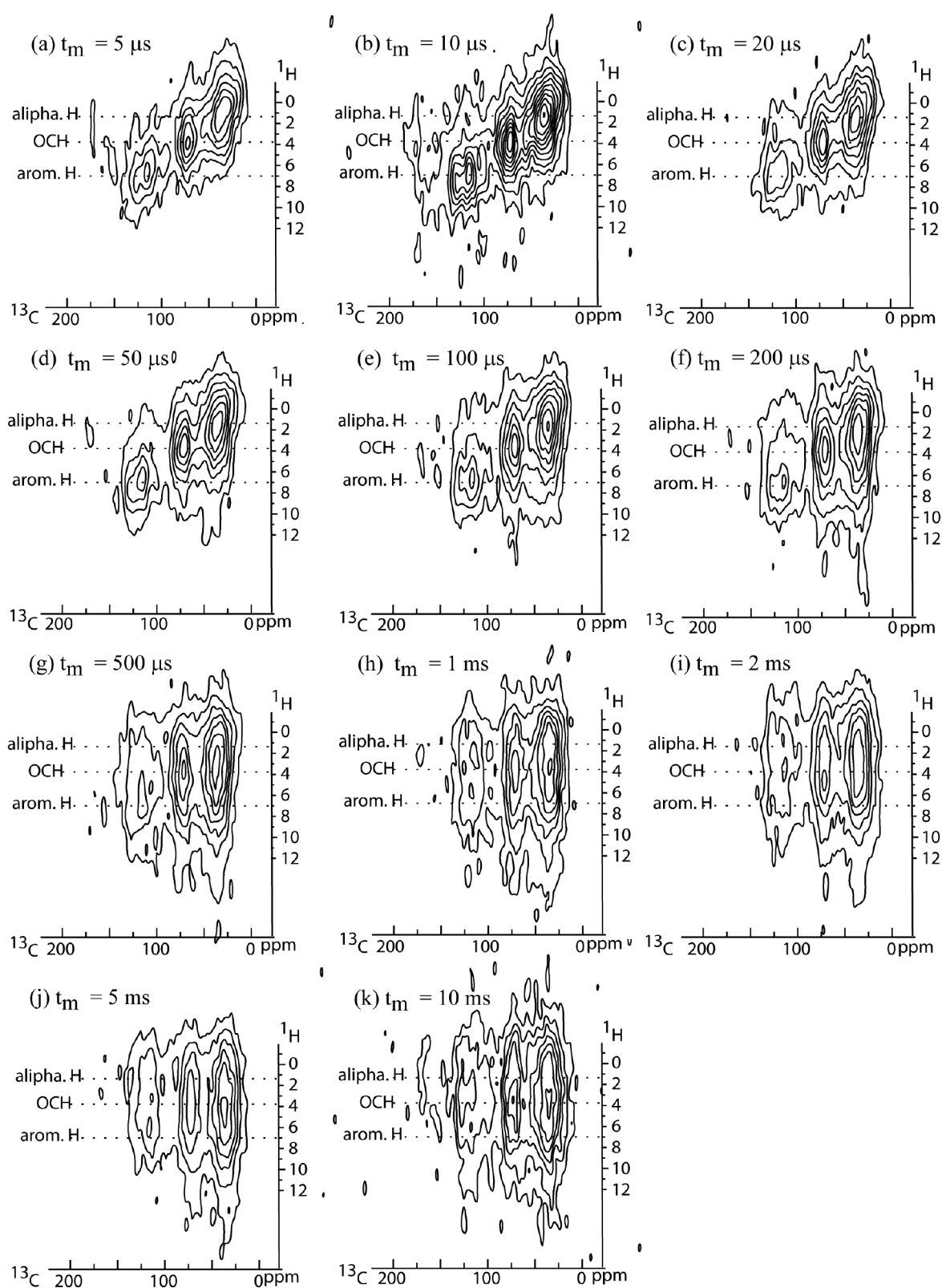


**Fig. 5.**  $^1\text{H}$ - $^{13}\text{C}$  2D HETCOR with various mixing times of IHSS Suwannee River HA: (a)  $t_m = 5 \mu\text{s}$ , (b)  $t_m = 10 \mu\text{s}$ , (c)  $t_m = 20 \mu\text{s}$ , (d)  $t_m = 50 \mu\text{s}$ , (e)  $t_m = 100 \mu\text{s}$ , (f)  $t_m = 200 \mu\text{s}$ , (g)  $t_m = 500 \mu\text{s}$ , (h)  $t_m = 1 \text{ ms}$ , (i)  $t_m = 2 \text{ ms}$ , (j)  $t_m = 5 \text{ ms}$ , (k)  $t_m = 10 \text{ ms}$ .



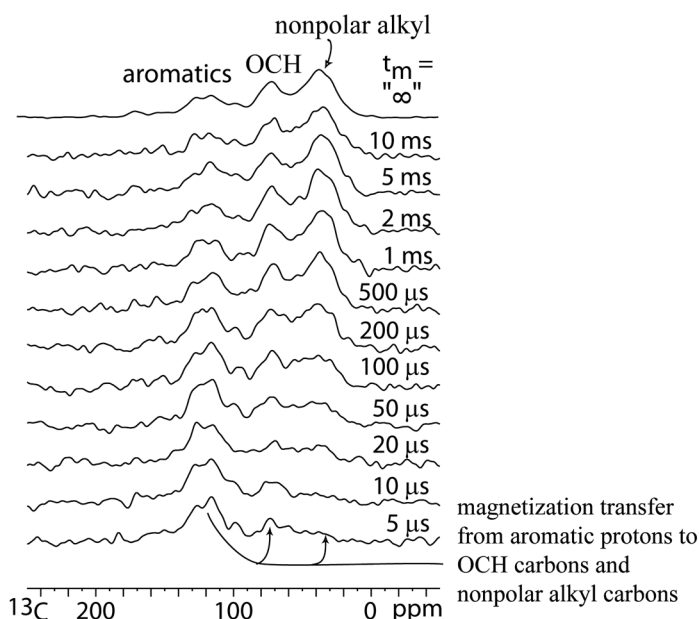


**Fig. 6.**  $^1\text{H}$  spin diffusion slices extracted from  $^1\text{H}$ - $^{13}\text{C}$  2D HETCOR spectra in Fig. 5, taken at the aromatic protons around 7.5 ppm.

scans, a series of 2D HETCOR spectra with various mixing times (around 10 2D HETCOR spectra) will take 4–5 days.

## Discussion

Using the 2D HETCOR with  $^1\text{H}$  spin diffusion technique and via calibration by the  $^1\text{H}$  spin-diffusion data of model polymers, we found only heterogeneities in the three NOM samples. The formation mechanisms of NOM have been in debate for many years (Stevenson 1994). Various mechanisms have been proposed, such as selective preservation (Philp and Calvin 1976; Hatcher et al. 1983) and depolymerization-condensation (Stevenson 1994). According to the traditional view, humic substances are refractory polymers. However, the more recent view indicates that they are regarded as being composed of diverse, relatively low molecular mass components that form dynamic associations and are stabilized by hydrophobic interactions and hydrogen bonds (Piccolo 2001; Sutton and Sposito 2005).

With this new  $^1\text{H}$  spin diffusion technique, we can examine these concepts and mechanisms with a new perspective. As stated in the "Introduction," if some biopolymers are selectively preserved, the partial survival of biomacromolecules would result in heterogeneities on a  $>1\text{-nm}$  scale. In contrast, the decomposition of biopolymers into short oligomers, followed by random repolymerization could lead to the intimate mixing of components and therefore heterogeneities  $< 1\text{ nm}$ . Based on the new view on humic substances, we also expect to observe heterogeneities  $< 1\text{ nm}$  in humic substances. For the three NOM samples, we only observe heterogeneities, excluding selective preservation pathway as the dominant formation

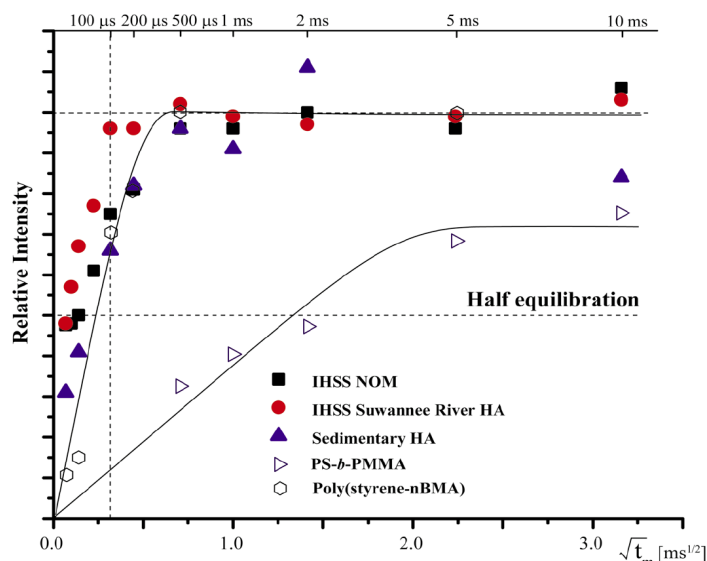


**Fig. 7.**  $^1\text{H}$  spin diffusion curves showing the plot of the peak intensities of OCH groups in the cross-sections shown in Fig. 6 as a function of the square root of the spin-diffusion time  $t_m$ . For calibration, the spin diffusion data of two model polymers, a synthetic random copolymer poly(styrene-*n*BMA) and a 50:50 block copolymer PS-*b*-PMMA, are included. Squares: IHSS NOM; circles: IHSS Suwannee River HA; filled triangles: sedimentary HA; open hexagons: poly(styrene-*n*BMA); and open left-sided triangles: PS-*b*-PMMA.

mechanism. The results are consistent with the concept that humic substances are inherently heterogeneous (MacCarthy 2001).

We only use three NOM samples to demonstrate the new  $^1\text{H}$  spin diffusion technique in the present study. Therefore, although our results are consistent with the depolymerization-repolymerization theory and the new view of humic substances, other formation mechanisms cannot be refuted considering that NOM from different environments may be formed via different mechanisms. Therefore, a systematic study on carefully selected NOM samples from different environments will be needed in the future so that we can provide a clearer picture for this puzzling, long-debating question—the formation mechanisms of NOM. This new technique opens a new avenue not only for exploring the mechanisms of NOM formation but also for exploring NOM interactions with other chemical species. For example, the structural information on domain and heterogeneities is closely related to sorption of nonpolar organic contaminants because significant sorption of nonpolar contaminants requires nonpolar domains. This has significant implications for sorption mechanism of nonpolar organic contaminants in soil and clean-up options (Mao and Schmidt-Rohr 2006).

## Comments and recommendations

The critical aspect of this technique is to achieve the clean suppression of one functional group so that the transfer of

magnetization can be quantitatively and reliably estimated. If necessary, overlap-induced artifacts can be suppressed by combining HETCOR with a  $^1\text{H}$  chemical shift filter or  $^{13}\text{C}$  chemical shift filter to reduce the undesirable strong peaks. The revised pulse sequence is shown in Fig. 2b. A  $^1\text{H}$  chemical shift filter can be inserted before the  $^1\text{H}$   $90^\circ$  pulse to suppress OCH peak to reduce peak overlap (Schmidt-Rohr and Mao 2002). The  $^{13}\text{C}$  chemical shift filter (Mao and Schmidt-Rohr 2004), which selects  $\text{sp}^3$ -hybridized carbons, can be inserted before TOSS so that  $\text{sp}^3$ -hybridized anomeric OCO groups can be examined (Mao and Schmidt-Rohr 2004). More detailed descriptions on the  $^1\text{H}$  chemical shift filter can be found elsewhere (Clauss et al. 1993; Schmidt-Rohr and Mao 2002).

This technique is not only applicable to aquatic and sedimentary organic matter but also to other NOM samples. In the present study, we primarily focused on the aromatic and OCH proton resonances. However, for samples that do not contain carbohydrates, different focuses and slices should be chosen. For example, for old geological samples such as coal and kerogen that contain generally two bands of aromatics and alkyls, carbon slices from alkyl H or aromatic H should be extracted.

## References

- Abdulla, H. A. N., E. C. Minor, R. F. Dias, and P. G. Hatcher. 2010. Changes in the compound classes of dissolved organic matter along an estuarine transect: A study using FTIR and C-13 NMR. *Geochim. Cosmochim. Acta* 74:3815-3838 [doi:10.1016/j.gca.2010.04.006].
- Botto, R. E., R. Wilson, and R. E. Winans. 1987. Evaluation of the reliability of solid  $^{13}\text{C}$  NMR spectroscopy for the quantitative analysis of coals: study of whole coals and maceral concentrates. *Energy Fuels* 1:173-181 [doi:10.1021/ef00002a006].
- Clauss, J., K. Schmidt-Rohr, and H. W. Spiess. 1993. Determination of domain sizes in heterogeneous polymers by solid-state NMR. *Acta Polym.* 44:1-17 [doi:10.1002/actp.1993.010440101].
- Conte, P., and A. Piccolo. 1999. Conformational arrangement of dissolved humic substances. Influence of solution composition on association of humic molecules. *Environ. Sci. Technol.* 33:1682-1690 [doi:10.1021/es9808604].
- , R. Spaccini, and A. Piccolo. 2004. State of the art of CP/MAS C-13-NMR spectroscopy applied to natural organic matter. *Prog. Nucl. Magn. Reson.* 44:215-223 [doi:10.1016/j.pnmrs.2004.02.002].
- Cook, R. L. 2004. Coupling NMR to NOM. *Anal. Bioanal. Chem.* 378:1484-1503 [doi:10.1007/s00216-003-2422-z].
- Dixon, W. T. 1982. Spinning-sideband-free and spinning-sideband-only NMR spectra in spinning samples. *J. Chem. Phys.* 77:1800-1809 [doi:10.1063/1.444076].
- Gogou, A., and D. J. Repeta. 2010. Particulate-dissolved transformations as a sink for semi-labile dissolved organic matter: Chemical characterization of high molecular weight dissolved and surface-active organic matter in seawater and in diatom cultures. *Mar. Chem.* 121:215-223 [doi:10.1016/j.marchem.2010.05.001].
- Hatcher, P. G., E. C. Spiker, N. M. Szeverenyi, and G. E. Maciel. 1983. Selective preservation and origin of petroleum-forming aquatic kerogen. *Nature* 305:498-501 [doi:10.1038/305498a0].
- , K. J. Dria, S. Kim, and S. W. Frazier. 2001. Modern analytical studies of humic substances. *Soil Sci.* 166:770-794 [doi:10.1097/00010694-200111000-00005].
- Hedges, J. I., and others. 2000. The molecularly-uncharacterized component of nonliving organic matter in natural environments. *Org. Geochem.* 31:945-958 [doi:10.1016/S0146-6380(00)00096-6].
- Hu, W. G., J. D. Mao, B. S. Xing, and K. Schmidt-Rohr. 2000. Poly(methylene) crystallites in humic substances detected by nuclear magnetic resonance. *Environ. Sci. Technol.* 34:530-534 [doi:10.1021/es990506l].
- Maccarthy, P. 2001. The principles of humic substances. *Soil Sci.* 166:738-751 [doi:10.1097/00010694-200111000-00003].
- Mao, J. D., and K. Schmidt-Rohr. 2004. Separation of aromatic-carbon  $^{13}\text{C}$  NMR signals from di-oxygenated alkyl bands by a chemical-shift-anisotropy filter. *Solid State Nucl. Magn. Reson.* 26:36-45 [doi:10.1016/j.ssnmr.2003.09.003].
- and ———. 2005. Methylene spectral editing in solid-state C-13 NMR by three-spin coherence selection. *J. Magn. Reson.* 176:1-6 [doi:10.1016/j.jmr.2005.04.016].
- and ———. 2006. Absence of mobile carbohydrate domains in dry humic substances proven by NMR, and implications for organic-contaminant sorption models. *Environ. Sci. Technol.* 40:1751-1756 [doi:10.1021/es0511467].
- , R. M. Cory, D. M. Mcknight, and K. Schmidt-Rohr. 2007a. Characterization of a nitrogen-rich fulvic acid and its precursor algae from solid state NMR. *Org. Geochem.* 38:1277-1292 [doi:10.1016/j.orggeochem.2007.04.005].
- , L. Tremblay, J. P. Gagne, S. Kohl, J. Rice, and K. Schmidt-Rohr. 2007b. Humic acids from particulate organic matter in the Saguenay Fjord and the St. Lawrence Estuary investigated by advanced solid-state NMR. *Geochim. Cosmochim. Acta* 71:5483-5499 [doi:10.1016/j.gca.2007.09.022].
- , X. W. Fang, Y. Q. Lan, A. Schimmelmarmann, M. Mastalerz, L. Xu, and K. Schmidt-Rohr. 2010. Chemical and nanometer-scale structure of kerogen and its change during thermal maturation investigated by advanced solid-state  $^{13}\text{C}$  NMR spectroscopy. *Geochim. Cosmochim. Acta* 74:2110-2127 [doi:10.1016/j.gca.2009.12.029].
- Mehring, M. 1983. Principles of high resolution NMR in solids. Springer-Verlag.
- Nanny, M. A., R. A. Minear, and J. A. Leenheer. 1997. Nuclear magnetic resonance spectroscopy in environmental chemistry. Oxford Univ. Press.
- Philp, R. P., and M. Calvin. 1976. Possible origin for insoluble organic (kerogen) debris in sediments from insoluble cell-wall materials of algae and bacteria. *Nature* 262:134-136 [doi:10.1038/262134a0].

- Piccolo, A. 2001. The supramolecular structure of humic substances. *Soil Sci.* 166:810-832 [doi:10.1097/00010694-200111000-00007].
- Pines, A., M. G. Gibby, and J. S. Waugh. 1973. Proton-enhanced NMR of dilute spins in solids. *J. Chem. Phys.* 59:569-590 [doi:10.1063/1.1680061].
- Preston, C. M. 1996. Applications of NMR to soil organic matter analysis: History and prospects. *Soil Sci.* 161:144-166 [doi:10.1097/00010694-199603000-00002].
- Schmidt, F., M. Elvert, B. P. Koch, M. Witt, and K. U. Hinrichs. 2009. Molecular characterization of dissolved organic matter in pore water of continental shelf sediments. *Geochim. Cosmochim. Acta* 73:3337-3358 [doi:10.1016/j.gca.2009.03.008].
- Schmidt-Rohr, K., and H. W. Spiess. 1994. Multidimensional solid-state NMR and polymers. Academic Press.
- , and J. D. Mao. 2002. Efficient CH-group selection and identification in C-13 solid-state NMR by dipolar DEPT and H-1 chemical-shift filtering. *J. Am. Chem. Soc.* 124:13938-13948 [doi:10.1021/ja027362m].
- Stephens, B. M., and E. C. Minor. 2010. DOM characteristics along the continuum from river to receiving basin: a comparison of freshwater and saline transects. *Aquat. Sci.* 72:403-417 [doi:10.1007/s00027-010-0144-9].
- Stevenson, F. J. 1994. *Humus chemistry: genesis, composition, reactions.* John Wiley & Sons.
- Sutton, R., and G. Sposito. 2005. Molecular structure in soil humic substances: The new view. *Environ. Sci. Technol.* 39:9009-9015 [doi:10.1021/es050778q].
- Swift, R. S. 1996. Organic matter characterization, p. 1011-1069. *In* D. L. Sparks [ed.], *Methods of soil analysis.* Soil Science Society of America and American Society of Agronomy.
- Tremblay, L., and J. P. Gagne. 2007. Distribution and biogeochemistry of sedimentary humic substances in the St. Lawrence Estuary and the Saguenay Fjord, Quebec. *Org. Geochem.* 38:682-699 [doi:10.1016/j.orggeochem.2006.11.003].
- Wakeham, S. G., C. Lee, J. I. Hedges, P. J. Hernes, and M. L. Peterson. 1997. Molecular indicators of diagenetic status in marine organic matter. *Geochim. Cosmochim. Acta* 61:5363-5369 [doi:10.1016/S0016-7037(97)00312-8].

Submitted August 2011

Revised 9 September 2011

Accepted 14 October 2011